INFECTION AND IMMUNITY, Sept. 2005, p. 5301–5310 Vol. 73, No. 9
0019-9567/05/$08.00+0 doi:10.1128/IAI.73.9.5301–5310.2005

Cytotoxic Necrotizing Factor Type 1 Production by Uropathogenic *Escherichia coli* Modulates Polymorphonuclear Leukocyte Function

Jon M. Davis, Susan B. Rasmussen, and Alison D. O'Brien*

Department of Microbiology and Immunology, Uniformed Services University of the Health Sciences, Bethesda, Maryland 20814-4799

Received 21 March 2005/Returned for modification 20 April 2005/Accepted 12 May 2005

Many strains of uropathogenic *Escherichia coli* (UPEC) produce cytotoxic necrotizing factor type 1 (CNF1), a toxin that constitutively activates the Rho GTPases RhoA, Rac1, and Cdc42. We previously showed that CNF1 contributes to the virulence of UPEC in a mouse model of ascending urinary tract infection and a rat model of acute prostatitis and that a striking feature of the histopathology of the mouse bladders and rat prostates infected with CNF1-positive strains is an elevation in levels of polymorphonuclear leukocytes (PMNs). We also found that CNF1 synthesis leads to prolonged survival of UPEC in association with human neutrophils. Here, we tested the hypothesis that CNF1 production by UPEC diminishes the antimicrobial capacity of mouse PMNs by affecting phagocyte function through targeting Rho family GTPases that are critical to phagocytosis and the generation of reactive oxygen species. We found that, as with human neutrophils, CNF1 synthesis provided a survival advantage to UPEC incubated with mouse PMNs. We also observed that CNF1-positive UPEC down-regulated phagocytosis, altered the distribution of the complement receptor CR3 (CD11b/CD18), enhanced the intracellular respiratory burst, and increased levels of Rac2 activation in PMNs. From these results, we conclude that modulation of PMN function by CNF1 facilitates UPEC survival during the acute inflammatory response.

Urinary tract infections rank high among the most common types of symptomatic infections in humans (10, 31). Indeed, more than 6 million cases of cystitis, i.e., urinary tract infections that are restricted to the bladder, occur annually in the United States with an estimated health care cost of over $1 billion (31). Uropathogenic *Escherichia coli* (UPEC) are responsible for the majority of urinary tract infections and account for 85% to 95% of all cystitis isolates (31). Nearly twice as many women as men are seen by physicians for symptomatic urinary tract infection, and 40 to 50% of women experience at least one urinary tract infection in their lifetime (10). Long-term complications of urinary tract infection are rare; however, an ascending urinary tract infection can result in pyelonephritis and septicemia (16, 21).

The pathogenesis of *E. coli*-mediated urinary tract infection is not completely understood but likely involves the expression by the uropathogen of an array of virulence factors that facilitate colonization and evasion of the immune response. Type 1 fimbriae are established as UPEC virulence factors (8), while expression of other adhesins, such as P-pili and S-fimbriae, is strongly linked to UPEC pathogenicity (11). The precise role that α-hemolysin, a secreted toxin made by many UPEC isolates, plays in urovirulence is not understood. However, one possible explanation is that α-hemolysin changes host responses, a theory based on the finding that α-hemolysin modulates Ca^{2+} signaling in cultured primary renal epithelial cells (21). Cytotoxic necrotizing factor type 1 (CNF1) is often coproduced with α-hemolysin by UPEC strains (9) and, at least in vitro, it too mediates cellular effects (6) that result from alteration of host signaling molecules (23, 32).

Three sets of observations support a role for CNF1 in the pathogenesis of UPEC-mediated urinary tract infection or acute prostatitis. First, epidemiological data from Foxman (11), Blanco (2) and Goullet (13) suggest CNF1 is associated with increased virulence and the development of urinary tract infections. In support of these observations, Yamamoto and colleagues determined that 61% of UPEC isolates they tested carried the *cnf1* gene compared to fewer than 10% of the commensal isolates they assessed (36). Second, in a mouse model of ascending urinary tract infection, a CNF1-expressing UPEC, compared to its isogenic *cnf1* mutant, caused a greater acute inflammatory response in the bladder, colonized the bladder more extensively in a coinfection experiment, and survived better when coincubated with human neutrophils (30). Third, a rat model of acute prostatitis revealed that CNF1-expressing UPEC evoked more widespread gross inflammation of rat prostates in addition to more pronounced cellular infiltration by polymorphonuclear leukocytes (PMNs) than did the corresponding *cnf1* isogenic mutant (29).

CNF1, which was first described by Caprioli and colleagues (6), is an approximately 115-kDa single-chain AB toxin that catalyzes the deamidation of the catalytically active glutamine residue of the Rho family of GTPases. The Rho GTPases include at least 10 members, of which RhoA, Rac1, and Cdc42 are proven targets for CNF1 deamidation (22). These GTPases function as molecular switches that fluctuate between an active GTP-bound form and an inactive GDP-bound form. When the GTPases are bound to GTP they activate downstream targets

* Corresponding author. Mailing address: Department of Microbiology and Immunology, Uniformed Services University of the Health Sciences, B4052, 4301 Jones Bridge Road, Bethesda, MD 20814-4799. Phone: (301) 295-3400. Fax: (301) 295-3773. E-mail: aobrien@usuhs.mil.

such as kinases, and, when bound to GDP, the GTPases are inactive and sequestered in the cytosol. In this way, the Rho GTPases exert control over various cellular processes such as remodeling of the actin cytoskeleton (22), chemotaxis (12), and formation of membrane extensions (22). The deamidation of glutamine 63 in Rho and glutamine 61 in Rac and Cdc42 by CNF1 prevents the hydrolysis of GTP to GDP. This event results in the constitutive activation of Rho GTPases in CNF1 intoxicated cells.

Rho GTPases also play a central role in both phagocytosis and the generation of reactive oxygen species by PMNs (35). Specifically, phagocytosis of complement-opsonized bacteria requires activated Rho and the β_2-integrin CR3 (CD11b/CD18), while immunoglobulin G-mediated phagocytosis is dependent on FCγ receptors and both Cdc42 and Rac1 (7, 34). Moreover, generation of reactive oxygen species involves assembly of the NADPH oxidase complex in the phagocyte membrane. This enzyme complex consists of a membrane-bound flavocytochrome, cytosolic proteins, and Rac2 (3, 35). The precise role of Rac2 in NADPH oxidase assembly is not completely understood. However, the integral nature of Rac2 in efficient generation of reactive oxygen species was demonstrated in Rac2$^{-/-}$ mice (24) and supported by the multiple, rapidly progressing soft-tissue infections of a patient with a Rac2 point mutation that rendered the protein nonfunctional (1, 14, 20). In both cases, neutrophils from the host exhibited no or greatly reduced levels of reactive oxygen species generation following stimulation.

In this study, we tested the hypothesis that CNF1 expression by UPEC partially protects the organism against the antimicrobial properties of PMNs. We found that the CNF1 expressed by UPEC down-regulated phagocytosis, altered CD11b distribution on the PMN surface, and augmented the intracellular respiratory burst. These CNF1-induced phenotypic changes in PMNs culminated in enhanced net replication of CNF1-expressing UPEC and supports the hypothesis that CNF1 has a role in urinary tract infection pathogenesis by altering the innate immune response.

MATERIALS AND METHODS

Bacterial strains and growth conditions. UPEC isolate CP9 (pSX34LacZα), its isogenic derivative CP9*cnf1* (pSX34LacZα), and the complemented clone CP9*cnf1* (pHLK140) all previously described (30) were recreated for this study because the original clones were no longer available. (see section below) Expression of CNF1 by both wild-type and complemented mutant and the absence of CNF1 expression by the isogenic mutant was confirmed by Western blot analysis. Bacterial strains were grown overnight in Luria-Bertani (LB) broth supplemented with 50 μg/ml chloramphenicol at 37°C with shaking. An aliquot of the overnight growth was transferred to LB agar plates supplemented with 50 μg/ml chloramphenicol and grown overnight at 37°C. The bacteria were resuspended from the plates with 2 ml of Hanks balanced salt solution (HBSS, BioWhittaker) without Ca^{2+}, Mg^{2+}, or phenol red. The resulting suspension was diluted to an A_{600} of 0.7, corresponding to 6×10^7 CFU/ml of a log-phase culture. The suspension was further diluted 1:10 in HBSS supplemented with 100 μM Ca^{2+}, 100 μM Mg^{2+}, 0.1% gelatin, 100 μM glucose, and 50 μg/ml chloramphenicol (HBSS-A) prior to use.

Complementation of CP9*cnf1*. Plasmids pHLK140 and pSX34LacZα have been previously described (30). Electroporation of pSX34LacZα into CP9 or CP9*cnf1* yielded CP9 (pSX34LacZα), the wild-type with empty vector, and CP9*cnf1* (pSX34LacZα), the isogenic mutant with empty vector, respectively. The electroporation of pHLK140 into CP9*cnf1* yielded CP9*cnf1*(pHLK140), the complemented mutant. Transformants were selected on LB agar that contained 50 μg/ml chloramphenicol. A single chloramphenicol-resistant colony was selected from each plate for further analysis. Growth curves of the individual strains were constructed to ensure that all strains grew equally well and that expression of CNF1 was evident by Western blotting.

Serum sensitivity. Bacteria were tested for sensitivity to mouse serum by incubating the individual bacterial strains in Hank's balanced salt solution with various serum concentrations (2%, 5%, and 10%). The mixtures were rotated end-over-end at 37°C and aliquots taken at 0, 90, and 150 min to determine bacterial viability by plating serial dilutions in triplicate onto LB agar supplemented with 50 μg/ml chloramphenicol. Following overnight growth, the number of colonies on each plate was counted and the concentration in CFU/ml calculated. Controls run in parallel contained bacteria with all mixture components except serum.

PMN elicitation. Five-week-old female C3H/HeOuJ mice (Jackson Laboratory, Bar Harbor ME) were injected intraperitoneally with 2.5 ml 3% thioglycolate broth (Difco) and returned to their cages. The mice were euthanized by isoflurane overdose and cervical dislocation five hours postinjection. Seven milliliters of HBSS without Ca^{2+} or Mg^{2+} supplemented with 0.1% gelatin (HBSS-W) was instilled for peritoneal lavage of euthanized mice using a syringe and 18-gauge needle. The cells were centrifuged then pooled prior to determining the concentration of viable cells in a hemocytometer using trypan blue dye exclusion. An aliquot of the cell suspension was placed on a glass slide by a cytospin centrifuge (Cytospin II, Shandon), fixed with methanol and stained with SureStain Wright (Fisher). The percentage of PMNs in the peritoneal exudate cells was then determined visually using a 100× oil immersion objective on an Olympus microscope (BX60). The peritoneal exudate cells consisted of 92% granulocytes, 4% mononuclear cells, and 4% lymphocytes. The Uniformed Services University of the Health Sciences Institutional Animal Care and Use Committee approved all animal use protocols.

Bacterial survival. All reactions were conducted in 1-ml volumes using HBSS-A at 37°C with end-over-end rotation. Bacterial strains were added to individual polypropylene tubes at a concentration of 5×10^5 CFU/ml. The bacteria were opsonized in 10% normal mouse serum at 37°C prior to the addition of 2×10^6 PMNs. Control tubes included bacteria with an equal volume of HBSS-A in place of PMNs; the use of heat-inactivated serum (56°C for 45 min) in place of normal mouse serum; or cytochalasin D-treated PMNs. Cytochalasin D treatment was done according to the method of Rest and Speert (28). The number of viable bacteria at 0, 90, and 150 min was determined by plate count as above. PMN viability was checked by trypan blue dye exclusion at the end of the assay.

Bacterial association with PMNs. PMNs and bacteria were prepared as described above and coincubated for 90 and 150 min at 37°C with end-over-end rotation. An aliquot was taken and affixed to a glass slide using a cytospin centrifuge. Each slide was stained using SureStain Wright (Fisher), and the number of bacteria associated with 100 total PMNs was determined microscopically. Due to the method of staining, it was not possible to discriminate intracellular from extracellular bacteria, and, therefore, the results are reported as the total number of PMN-associated bacteria.

PMN phagocytic capacity. PMNs (10^6) were allowed to adhere to glass coverslips coated with 3 mg/ml poly-D-lysine (Sigma P-0899) in 24 well cell culture dishes. Nonadherent cells were washed away, and preopsonized bacteria were then added at a multiplicity of infection of 1:1. The PMNs and bacteria were coincubated for 90 or 150 min and washed to remove nonadherent bacteria. The PMN-bacteria mixtures were fixed with fresh 3.5% paraformaldehyde (Electron Microscopy Services 15710) for 30 min at 37°C. The fixed infected PMNs were then washed in phosphate-buffered saline and incubated overnight at 4°C in blocking buffer that contained 3% bovine serum albumin (Sigma A-4503) and 10% heat-inactivated normal goat serum (Sigma G-9023). Extracellular bacteria were labeled by incubation for 1 h at room with rabbit anti-O4 polyclonal serum (Centers for Disease Control) diluted 1:200 in blocking buffer. The fixed infected PMNs were then washed in phosphate-buffered saline to remove unbound primary antibody, and the secondary antibody, goat anti-rabbit Alexa 594 (Molecular Probes) 5 μg/ml in blocking buffer, was applied for 1 h at room temperature.

The infected PMNs with labeled extracellular bacteria were again fixed in fresh 3.5% paraformaldehyde for 30 min at room temperature. Following an additional wash, the cells were permeabilized by treatment with 0.3% Triton X-100 for 3 min and then washed in phosphate-buffered saline. The cells were incubated overnight in blocking buffer at 4°C. Intracellular bacteria were then labeled following the same labeling protocol used for extracellular bacteria except that the secondary antibody was changed to goat anti-rabbit Alexa 488 (Molecular Probes). The cells were observed on an Olympus microscope (model BX60) equipped for epifluorescence with filters for fluorescein isothiocyanate (Chroma Technologies, set 41001) and tetramethylrhodamine isothiocyanate (Chroma Technologies, set U-M41002). The phagocytic capacity of the PMNs was determined by counting the total number of intracellular bacteria contained within

100 PMNs. The percent of PMNs engaged in phagocytosis was determined by counting the number of PMNs that contained at least one intracellular bacterium per 100 total PMNs; the results were then multiplied by 100. For both sets of counts, at least four separate fields were analyzed by phase contrast imaging of PMNs visualized with a 100× oil immersion lens.

CD11b staining. PMNs and bacteria were coincubated under the same conditions used to determine phagocytic capacity. Following coincubation, nonadherent bacteria were removed by washing and the cells were blocked overnight at 4°C in blocking buffer. Goat anti-mouse Alexa 488 CD11b (Pharmingen) 5 μg/ml and rabbit polyclonal α-O4 diluted 1:200 were applied in blocking buffer for 1 h at room temperature to label CD11b and adherent bacteria, respectively. After washing, goat anti-rabbit Alexa 594 (Molecular Probes) was applied at 5 μg/ml for 1 h at room temperature and subsequently washed. The cells were fixed for 30 min at room temperature in 3% freshly prepared paraformaldehyde (EMS) and washed in phosphate-buffered saline before mounting the coverslips on glass slides using Fluoromount G (Southern Biotech). Images were acquired on a Zeiss LSM 5 PASCAL confocal microscope using a 100× oil lens (NA 1.4) and analyzed using the LSM 5 PASCAL software.

Nitroblue tetrazolium reduction. PMNs (10^6) were preincubated for 5 min with a 50 μg/ml solution of nitroblue tetrazolium in dimethyl sulfoxide at 37°C in polypropylene tubes. Preopsonized bacteria (10^6) were added to the PMNs and rotated end over end at 37°C. Samples were taken at 0, 15, and 30 min; the shorter time points were selected for this assay because of artifactual reduction of nitroblue tetrazolium at time points beyond 30 min. PMNs incubated without bacteria served as background controls. Samples were affixed to glass slides using a cytospin centrifuge and fixed with methanol. The cells were counter stained with Safranin O following fixation and air-dried. The percent of PMNs that contained purple formazan crystals from reduced nitroblue tetrazolium was determined on a light microscope (Olympus BX60) using a 100× oil immersion objective.

Luminol/isoluminol-enhanced chemiluminescence. Luminol-enhanced chemiluminescence was used to measure the presence of intracellular reactive oxygen products and isoluminol-enhanced chemiluminescence was used to detect the presence of extracellular reactive oxygen products. Both reactions were conducted in duplicate in 96-well microtiter plates at 37°C with periodic gentle shaking in a luminometer (Fluoroskan Ascent FL, Thermo Labsystems) according to the method of Bylund (5). We verified that we could detect intracellular and extracellular reactive oxygen species under our assay conditions by stimulating PMNs with phorbol myristate acetate (Sigma) or formyl-Met-Leu-Phe (Sigma). Preopsonized bacteria were added to duplicate wells of the microtiter plate and the light emission was recorded every minute for 150 min with Ascent software (Labsystems version 2.4.2). The raw data collected by the Ascent software were exported into Excel (Microsoft Corp.), and peak and time to peak values were determined.

Rac activation assay. PMNs (2×10^6) and preopsonized bacteria (2×10^7) were coincubated in HBSS-A with 10% mouse serum for 150 min in a total volume of 1 ml. The extent of Rac2 activation was determined by the Rac activation assay from Upstate Biological according to the manufacturer's protocol. The sample portion not used for affinity precipitation was retained for use as an internal control to verify equivalent loading of lanes.

Western blotting. CNF1 in mixtures of individual strains of bacteria coincubated with PMNs for 150 min was detected by immunoblot as follows. Sonic lysates of the PMN-bacteria mixtures were prepared by pulsing samples on wet ice with a Sonic Dismembrator 550 (Fisher Scientific) for 3 min (30 seconds on, 30 seconds off). Proteins were resolved on 6.5% sodium dodecyl sulfate-polyacrylamide gel electrophoresis (SDS-PAGE) gels and transferred to nitrocellulose membranes in a semidry apparatus (Bio-Rad). Protein-containing membranes were blocked overnight in a blocking buffer that consisted of 5% (wt/vol) skim milk in Tris-buffered saline with 0.1% Tween 20 (TBS-T), and the membranes were then probed with goat anti-CNF1 serum, diluted 1:10,000 and prepared as described previously (26). These blots were then incubated with a horseradish peroxidase-conjugated secondary pig anti-goat (1:10,000) (Bio-Rad) in blocking buffer. Affinity-precipitated or total Rac2 was resolved on 12% SDS-PAGE. Following transfer to nitrocellulose membranes and overnight blocking, the membranes were probed with rabbit polyclonal anti-Rac-2 (1:400) (Santa Cruz Biotechnology) in blocking buffer. Blots were then incubated with HRP-conjugated secondary goat anti-rabbit (1:4,000) (Bio-Rad) in blocking buffer. Visualization of both CNF1 and Rac2 was accomplished by enhanced chemiluminescence (ECL PLUS, Amersham).

Flow cytometry. PMNs were evaluated for CD11b expression by washing cells with fluorescence-activated cell sorting buffer (Dulbecco's phosphate-buffered saline plus 0.2% fetal bovine serum plus 0.1% sodium azide) after coincubation with bacteria. PMNs were washed and resuspended in 100 μl of fluorescence-activated cell sorting buffer and blocked with 1 μg rat anti-mouse CD16/CD32 monoclonal antibody 2.4G2 (Pharmingen) for 20 min at room temperature. PMNs were then washed twice in fluorescence-activated cell sorting buffer and resuspended in 100 μl fluorescence-activated cell sorting buffer. Cells were stained on ice for 30 min with 0.5 μg/ml peridinin chlorophyll protein- and Cy5.5-labeled rat anti-mouse CD11b monoclonal antibody clone M1/70 (Pharmingen) and 0.8 μg/ml phycoerythrin-labeled rat anti-mouse Gr-1 monoclonal antibody clone 1A8 (Pharmingen). Cells were washed and resuspended in fluorescence-activated cell sorting buffer with 0.4% paraformaldehyde (EMS). Isotype-matched controls were run in parallel. Gating was set on Gr-1-positive cells and 30,000 events were collected on an LSR II flow cytometer (Becton-Dickenson), and analyzed using WinList software v 5.0.

Statistical analysis. All calculations were performed using Statistical Package for the Social Sciences 11.0 (SPSS 11.0) in consultation with our in-house statistician, Cara Olsen. Nonparametric data were evaluated for statistical significance using the Mann-Whitney U-test. Parametric data were evaluated by analysis of variance after the residuals were plotted to determine that the data were normally distributed.

RESULTS

CNF1 enhances UPEC replication in the presence of murine PMNs. We previously showed that wild-type UPEC strain CP9 survived better than the corresponding isogenic mutant CP9*cnf1* after 45 min of contact with human neutrophils (30). To extend and further characterize the impact of CNF1 expression on the interaction between these phagocytes and UPEC, we compared the growth of the wild-type strain, the CNF1-negative mutant, and the complemented clone in the presence of elicited peritoneal exudate cells (92% granulocytes, hereafter called PMNs) from C3H/HeOuJ mice. This mouse strain was selected because of its use in our previously published studies on the role of CNF1 in the ascending urinary tract infection model (30).

The CP9-derived derivatives used in this investigation included the wild-type strain transformed with the cloning vector alone [CP9(pSX34LacZα)], the isogenic CNF1-negative mutant also transformed with the cloning vector alone [CP9*cnf1*(pSX34LacZα)], and the complemented mutant of CP9*cnf1* [CP9*cnf1*(pHLK140)], that was previously described (30) but freshly transformed for this study. Western blot analysis confirmed the presence of CNF1 in the wild type and complemented clone, but no CNF1 was detected in the mutant (data not shown). The growth curves of these three strains in medium without PMNs were superimposable (data not shown). By contrast, when we compared the net replication of CP9(pSX34LacZα) (hereafter called the wild type or the wild-type strain), CP9*cnf1*(pSX34LacZα) (hereafter called the mutant or the isogenic mutant) and CP9*cnf1*(pHLK140) (hereafter called the complemented mutant) after coincubation with C3H/HeOuJ PMNs, both the wild-type and the complemented mutant grew to a significantly greater extent ($P < 0.01$) than did the mutant after 90 min (Fig. 1A). Moreover, the wild-type strain and the complemented mutant in the presence of the murine PMNs continued to demonstrate significantly ($P < 0.01$) greater net replication throughout the 150 min of the assay, while the isogenic mutant failed to undergo any significant net growth (Fig. 1A). A Western blot of the assay mixtures demonstrated that CNF1 was produced under the conditions of our experiment (Fig. 1B). Control experiments using PMNs treated with cytochalasin D, a known inhibitor of actin polymerization and phagocytosis, resulted in all three bacterial strains growing equally well (Fig. 1C).

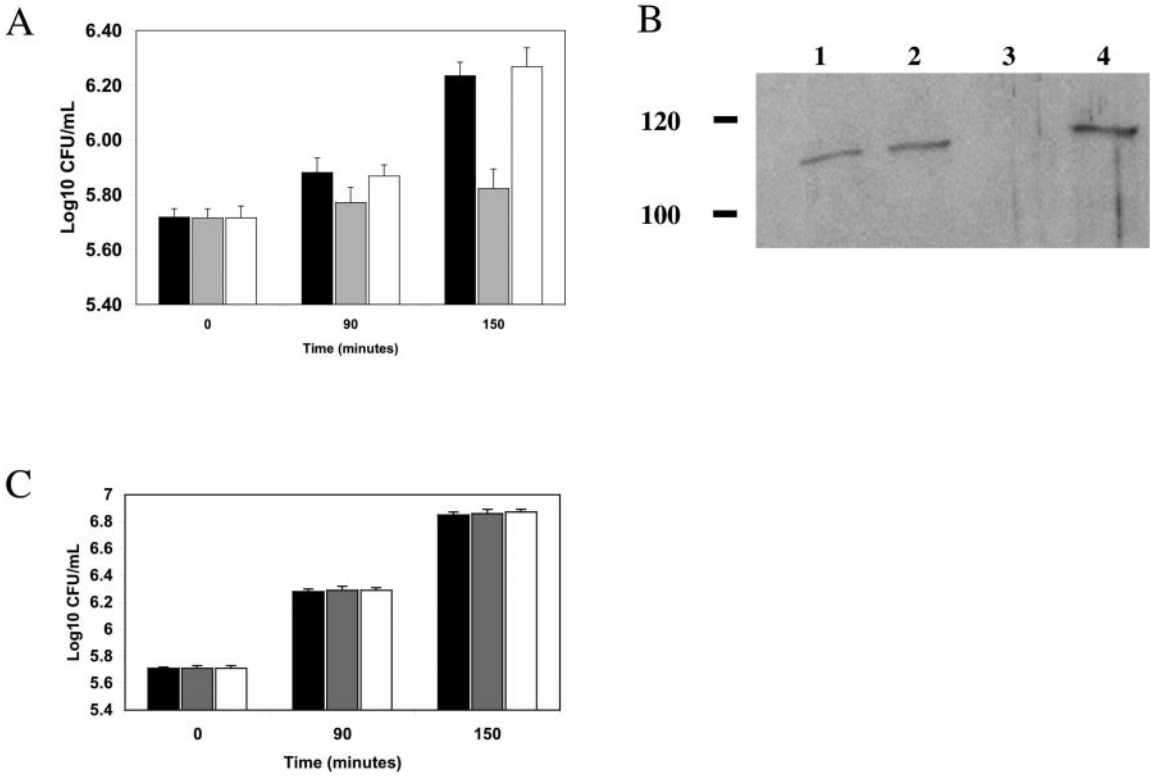

FIG. 1. Influence of untreated and cytochalasin D-treated PMNs on net replication of CNF1-positive and -negative UPEC. (A) Bacterial strains were coincubated with PMNs and viable bacteria were enumerated by plating serial dilutions at the indicated time points. Each bar represents the mean $\log_{10}$ CFU/ml of three independent experiments done in triplicate. Counts are presented for strains depicted as follows: wild-type CP9(pSX34LacZα), black; isogenic mutant CP9*cnf1*(pSX34LacZα), gray; and complemented mutant CP9(pHLK140), white. The error brackets indicate the 95% confidence interval for each determination. The data were analyzed by analysis of variance and differences are significant ($P < 0.01$). (B) Western blot analysis of CNF1 in sonically disrupted lysates of bacteria and PMNs after coincubation. Lane 1, purified CNF1; lane 2, lysate of wild-type CP9(pSX34LacZ); lane 3, lysate of isogenic mutant CP9*cnf1*(pSX34LacZ); lane 4, lysate of complemented mutant CP9*cnf1*(pHLK140). (C) PMNs were preincubated with cytochalasin D prior to adding UPEC and viable bacteria were enumerated by plating serial dilutions. Each bar represents the mean $\log_{10}$ CFU/ml of three independent experiments done in triplicate. Counts are presented for strains depicted as follows: CP9(pSX34LacZα), black; CP9*cnf1*(pSX34LacZα), gray; and CP9(pHLK140), white. The error brackets indicate the 95% confidence interval for each determination. The data were analyzed by analysis of variance and differences are significant ($P < 0.01$).

The results of this cytochalasin D experiment suggested that the growth differences observed among the three UPEC strains tested in the presence of PMNs (Fig. 1C) were due to an impairment of the phagocytic process, rather than the release of antimicrobial products from the PMNs into the extracellular environment. Additional control experiments using heat-inactivated serum as a source of opsonins also resulted in all three strains growing equally well; these results demonstrated that heat-labile factors are required for the observed growth differences (data not shown). Finally, to demonstrate that the three strains used were not sensitive to the concentration of normal mouse serum incorporated into the media in our experiments, all three strains were grown in the presence of 10% normal mouse serum without PMNs. Strains so cultivated demonstrated growth equivalent to strains cultured in the absence of serum (data not shown).

Collectively, these results show that CNF1-expressing UPEC have a growth advantage when coincubated with PMNs from peritoneal exudates of C3H/HeOuJ mice and support our previous findings that the CNF1-positive CP9 strain grew better in the presence of human neutrophils than did its CNF1-negative isogenic mutant. In addition, the findings with murine PMNs indicate that this CNF1-dependent differential growth is due to alteration in a phagocytic process that requires heat-labile serum factors.

PMN phagocytic capacity and CD11b clustering is altered in the presence of CNF1-expressing UPEC. Based on the results obtained in the bacterial survival experiments described above, we undertook a series of experiments to assess the extent of PMN association with the wild-type and the isogenic mutant. The number of wild-type bacteria associated with 100 PMNs was significantly increased compared to the isogenic mutant at 90 min (268 versus 173, $P < 0.05$, $n = 4$). The number of wild-type bacteria associated with PMNs reached a plateau after 150 min of coincubation while the mutant continued to associate in significantly greater numbers (259 versus 400, $P < 0.05$, $n = 4$). These data further support the suggestion from the cytochalasin D experiments above that CNF1-expression by CP9 modulates phagocytosis by PMNs.

Next, we conducted a set of studies that were designed to use differential immunolabeling as a tool to evaluate the phagocytic capacity of the infected C3H/HeOuJ PMNs and the percent of PMNs engaged in phagocytosis. The results of those experiments are shown in Table 1. When coincubated with

TABLE 1. Phagocytic capacity and activity of PMNs exposed to UPEC[a]

Strain	90 min		150 min	
	No. of bacteria/ 100 PMN	% phagocytosing PMN	No. of bacteria/ 100 PMN	% phagocytosing PMN
CP9 (pSX34LacZα)	141 (135–147)	15 (11–18)	123 (120–125)	8 (7–9)
CP9*cnf1*(pSX34LacZα)	230 (225–235)[b]	77 (71–80)[b]	262 (256–267)[b]	77 (71–81)[b]
CP9*cnf1*(pHLK140)	143 (138–150)	13 (11–15)	128 (124–133)	6 (4–7)

[a] Data are the median and range of four independent experiments, and strains are designated as follows: wild-type [CP9(pSX34LacZα)], mutant [CP9*cnf1*(pSX34LacZα)], and complemented mutant [CP9*cnf1*(pHLK140)].
[b] Significantly greater compared to wild-type and complemented mutant ($P < 0.01$).

CNF1-expressing UPEC, the phagocytic capacity of the murine PMNs was significantly diminished at both 90 and 150 min. The percent of PMNs that exhibited phagocytic activity when in contact with CNF1-expressing UPEC compared to the mutant was also significantly lower, and the phagocytic activity of these PMNs decreased over time.

The anti-phagocytic effect of CNF1 expressed by UPEC suggested that the PMNs were not interacting productively with serum-opsonized bacteria, perhaps due to failure to express or cluster complement receptor 3 (CR3, CD11b/CD18) on the PMN surface. To test this theory, we coincubated PMNs with each of the three strains (wild type, mutant, and complemented mutant) and analyzed the expression of CD11b on the PMN surface. Fluorescence-activated cell sorting analysis revealed that the level of CD11b expression on the surface of elicited mouse PMNs was unchanged regardless of the bacterial strain used in these coincubation experiments (data not shown). We then asked whether CNF1-expressing UPEC could influence the clustering of CD11b in response to serum-opsonized bacteria.

To address that question, PMNs that were coincubated with each of the bacterial strains were immunostained for both bacteria and CD11b and then examined by confocal microscopy. The results of this experiment are shown in Fig. 2. PMNs coincubated with the wild-type strain (Fig. 2, panel A i.) demonstrated a homogenous distribution of CD11b along the periphery of the leukocyte. Conversely, PMNs incubated with the CNF1-negative mutant exhibited dense regions of clustered CD11b localized mainly under bacteria (Fig. 2, panel A, ii). The distribution of CD11b on the PMNs in association with the complemented mutant (Fig. 2, panel A, iii) was like that of PMNs incubated with the wild-type strain. The change in fluorescence intensity of CD11b along a line segment extending from the point of UPEC attachment to the opposite side of the PMN provided a measure of the capacity of PMNs to cluster CD11b in response to serum-opsonized bacteria (Fig. 2A, profiles under immunostained PMNs). PMNs exposed to CNF1-expressing UPEC exhibited a significantly ($P < 0.01$) impaired capacity to cluster CD11b in response to serum-opsonized UPEC compared to PMNs exposed to the *cnf1* mutant (Fig. 2B).

We also observed that PMNs coincubated with CNF1-expressing UPEC appeared more compact than did PMNs exposed to the *cnf1* isogenic mutant. Indeed, when the area of PMNs exposed to each of the three strains was measured, we found that PMNs coincubated with CNF1-expressing UPEC showed a significantly ($P < 0.01$) reduced degree of spread compared to PMNs exposed to the isogenic mutant (Fig. 3). The results of these experiments taken collectively demonstrate that CNF1-expressing UPEC have an anti-phagocytic effect on mouse PMNs and suggest that the anti-phagocytic effect may result from the diminished capacity of PMNs to remodel their membranes and cluster CD11b in response to the presence of serum-opsonized bacteria.

CNF1-expressing UPEC modify the PMN respiratory burst. To examine whether or not PMNs coincubated with the different UPEC bacterial strains also exhibited an altered competence to generate reactive oxygen species, we first measured the PMN respiratory burst using nitroblue tetrazolium dye reduction. The percent of PMNs that contained formazan deposits was significantly greater when coincubated with CNF1-expressing UPEC than when mixed with the *cnf1* mutant (Table 2). To verify the nitroblue tetrazolium reduction results, we used a procedure that exploits luminol- or isoluminol-enhanced chemiluminescence to specifically measure the intracellular and extracellular accumulation of reactive oxygen species, respectively. When the peak and time to peak values of the isoluminol reactions were compared, no significant difference was detected in the extracellular accumulation of reactive oxygen species. However, when murine PMNs were coincubated with CNF1-expressing bacteria, the PMNs generated a significantly greater intracellular peak response in the luminol assay compared to the *cnf1* mutant (Table 2); no difference in the time to peak was detected.

CNF1-expressing UPEC stimulate expression of enhanced levels of activated Rac2 in PMNs. The role of the small GTPase Rac2 in the assembly of a functional NADPH oxidase in neutrophils was previously demonstrated by Kim and Dinauer (17). Since CNF1 targets small GTPases, one explanation for the increased intracellular levels of reactive oxygen species after exposure of PMNs to CNF1-expressing UPEC was that the toxin had activated Rac2 in those phagocytes. To evaluate this idea, we used an affinity precipitation assay and antibodies specific for Rac2 to determine the extent of Rac2 activation in PMNs exposed to our UPEC strains. As illustrated in Fig. 4, PMNs exposed to CNF1-expressing UPEC contained nearly twice as much activated Rac2 as did PMNs exposed to the *cnf1* mutant; the results from each group were normalized to unstimulated PMNs. Together, these results provide evidence that exposure to CNF1-expressing UPEC results in an increased level of activated Rac2 in mouse PMNs.

DISCUSSION

In this study, we observed that mouse PMNs displayed several changes in phenotype when exposed to CNF1 expressed by

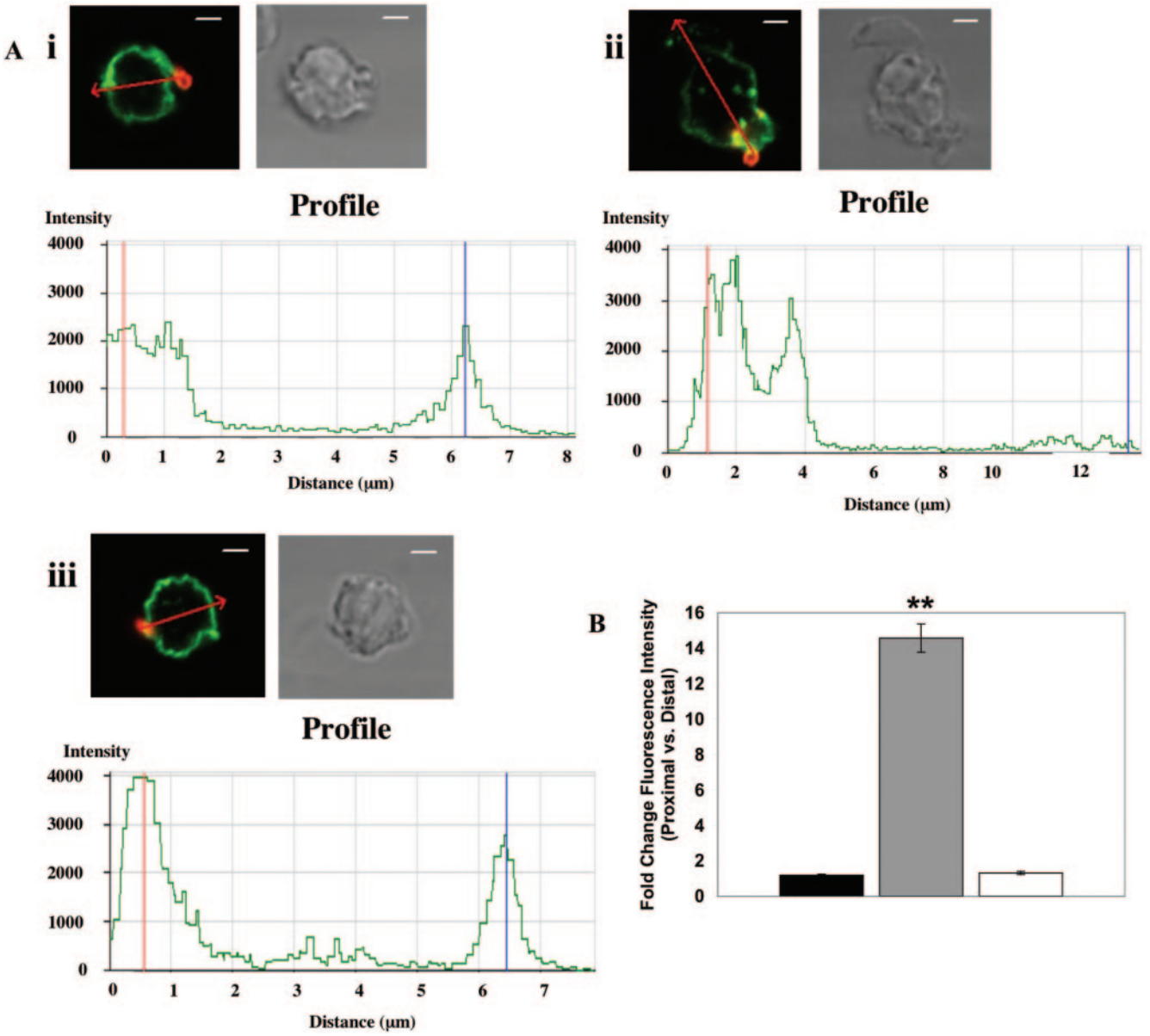

FIG. 2. Clustering of CD11b in mouse PMNs in contact with UPEC. (A) PMNs were coincubated with (i) wild-type CP9 (pSX34LacZα), (ii) isogenic mutant CP9*cnf1* (pSX34LacZα), or (iii) complemented mutant CP9*cnf1* (pHLK140) and confocal images were obtained following immunostaining for CD11b (green) and bacteria (red). PMNs coincubated with CNF1-expressing UPEC (i and iii) show a diffuse and approximately equal distribution of CD11b around the periphery of the cell compared to PMNs in contact with the *cnf1* mutant (ii) that demonstrate a clustering of CD11b beneath the bacteria. The CD11b pixel intensity along the red arrow extending from the point of UPEC attachment to a point on the opposite side of the PMN is shown in the profile plot under each image set. The red line in each profile plot indicates the intensity at the point of UPEC attachment and the blue line indicates the intensity at the opposite side of the phagocyte. Bar represents 2 μm. (B) Fold change of CD11b fluorescence intensity. The fluorescence intensity of CD11b directly under the UPEC was compared to the fluorescence intensity of CD11b on the opposite side of the PMN with the profile analysis tool in the LSM 5 PASCAL software. Each bar represents the mean fold increase in fluorescence intensity ($n = 30$); the brackets indicate the 95% confidence intervals. The bacterial strains used in the coincubation experiments are depicted as follows: wild-type CP9(pSX34LacZα), black; isogenic mutant CP9*cnf1*(pSX34LacZα), gray; and complemented mutant CP9(pHLK140), white. The data were analyzed by analysis of variance and differences are significant ($P < 0.01$).

UPEC. First, these PMNs showed decreased capacity to phagocytose CNF1-expressing bacteria compared to a CNF1-negative derivative. Second, exposure of PMNs to CNF1-positive UPEC resulted in redistribution of complement receptor 3 (CR3, CD11b/CD18) on the surface of the phagocyte and a diminished spreading of the PMNs. Third, CNF1 production by UPEC also altered the intracellular respiratory burst as measured by luminol. Fourth, the PMNs mixed with UPEC that expressed CNF1 demonstrated increased levels of activated Rac2, a Rho family GTPase involved in the assembly of the NADPH oxidase complex in PMNs. The net result of these CNF1-mediated phenotypic changes in PMNs was that CNF1-

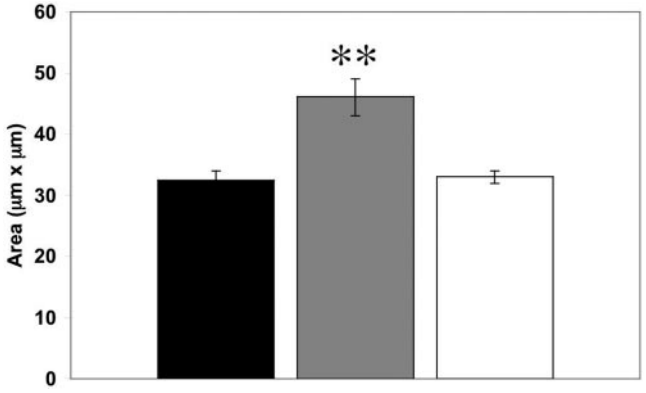

FIG. 3. PMN spreading in response to UPEC. PMNs were coincubated with each of the bacterial strains on glass coverslips coated with poly-D-lysine for 150 min. Following immunostaining for CD11b, confocal images were obtained. The area occupied by a PMN was calculated by tracing the PMN perimeter (as defined by the fluorescently labeled CD11b) with the measuring tool in the LSM5 PASCAL software. The data are shown as the mean and 95% confidence intervals ($n = 30$). The bacterial strains used in the coincubation experiments are represented as follows: CP9(pSX34LacZα), black; CP9*cnf1* (pSX34LacZα), gray; and CP9*cnf1*(pHLK140), white. The data were analyzed by analysis of variance and differences are significant ($P < 0.01$).

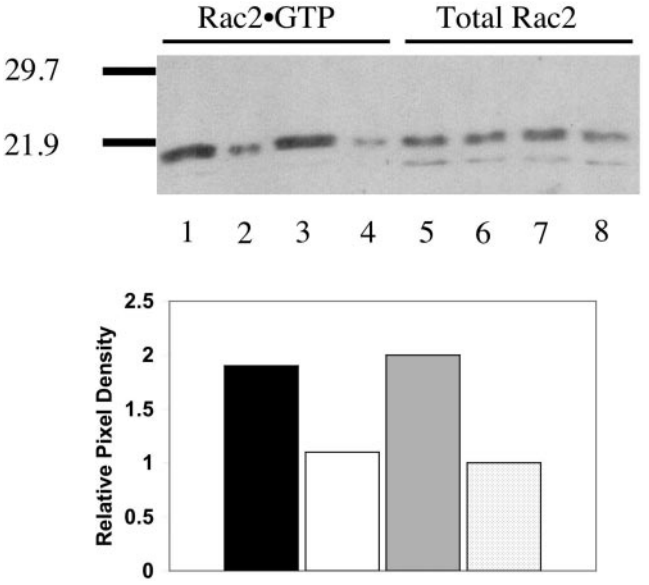

FIG. 4. Rac2 activation in PMNs coincubated with UPEC. (A) PMNs were incubated with each of the bacterial strains, and the activated form of Rac2 was affinity precipitated from whole cell lysates prior to detection by Western blotting. The unstimulated control contained PMNs only. The total Rac2 in whole cell lysates prior to affinity precipitation was used as a control to ensure that similar amounts of Rac2 were present. PMNs were exposed to CP9(pSX34LacZα) (lanes 1 and 5), CP9*cnf1*(pSX34LacZα) (lanes 2 and 6), CP9*cnf1*(pHLK140) (lane 3 and 7), or no bacteria (lanes 4 and 8) for 150 min prior to affinity precipitation. (B) The change in the amount of activated Rac2 compared to the unstimulated control was determined with Image J to quantify the pixel density of each lane. The data presented are representative of three separate experiments with similar results.

producing UPEC grew better in the presence of these phagocytes than did the isogenic CNF1-negative mutant. Such variation in net replication of CNF1-positive versus CNF1-negative UPEC in the presence of PMNs supports earlier observations from a mouse urinary tract infection model of coinfection in which the CNF1-expressing UPEC outcompeted the isogenic, CNF1-negative mutant in the bladder (30).

To explain our finding that CNF1-expressing UPEC were not phagocytosed as effectively as the isogenic mutant, and in light of previous studies that showed that CNF1 can alter the cytoskeleton of toxin-exposed cells (15, 23, 26, 32), we tested the idea that PMNs exposed to CNF1-positive UPEC are unable to remodel their plasma membranes. We reasoned that during phagocytosis, the neutrophil plasma membrane must adjust its shape in the region around the particle to be phagocytosed. Since the spreading of PMNs on surfaces requires the PMN plasma membrane to change contours, we used PMN spreading as a measure of such fluidity. We found that PMNs coincubated with CNF1-expressing UPEC failed to remodel their membrane, usually remained spherical in shape, and displayed significantly less spreading than did PMNs exposed to the *cnf1* isogenic mutant. Based on these observations, we conclude that the decreased plasticity of the plasma membrane of PMNs exposed to CNF1-expressing UPEC is in part responsible for the reduced phagocytic activity of those leukocytes.

Although the association of CNF1-expressing UPEC with PMNs was enhanced at early time points after infection, this association then reached a plateau. This observation suggests that available PMN receptors either were saturated or were not in the correct conformation to interact with or allow the PMNs to efficiently phagocytose serum-opsonized CNF1-expressing bacteria. We favor the first hypothesis. Indeed, if the

TABLE 2. Respiratory burst of PMNs exposed to UPEC

Strain	Nitroblue tetrazolium reduction[a] (% positive)		Luminol enhanced chemiluminescence[b]	
	15 min	30 min	Peak relative light units	Time to peak (min)
CP9(pSX34LacZα)	80 (79–83)	90 (87–97)	970 (654–1287)	47.5 (37.1–57.9)
CP9*cnf1*(pSX34LacZα)	62 (60–63)[c]	77 (67–77)[d]	452 (389–514)[e]	57.5 (33.5–81.5)
CP9*cnf1*(pHLK140)	87 (81–89)	94 (85–96)	920 (672–1168)	41.2 (36.7–45.6)

[a] Data are the median and range of three independent experiments, and strains are designated as follows: wild-type [CP9(pSX34LacZα)], mutant [CP9*cnf1*(pSX34LacZα)], and complemented mutant [CP9*cnf1*(pHLK140)].
[b] Values are shown as the mean and 95% confidence interval of three experiments in duplicate.
[c,d] Significantly less than wild-type or complemented mutant ($P = 0.05$), Mann-Whitney test.
[e] Significantly less than wild-type and complemented mutant ($P < 0.01$) as determined by analysis of variance.

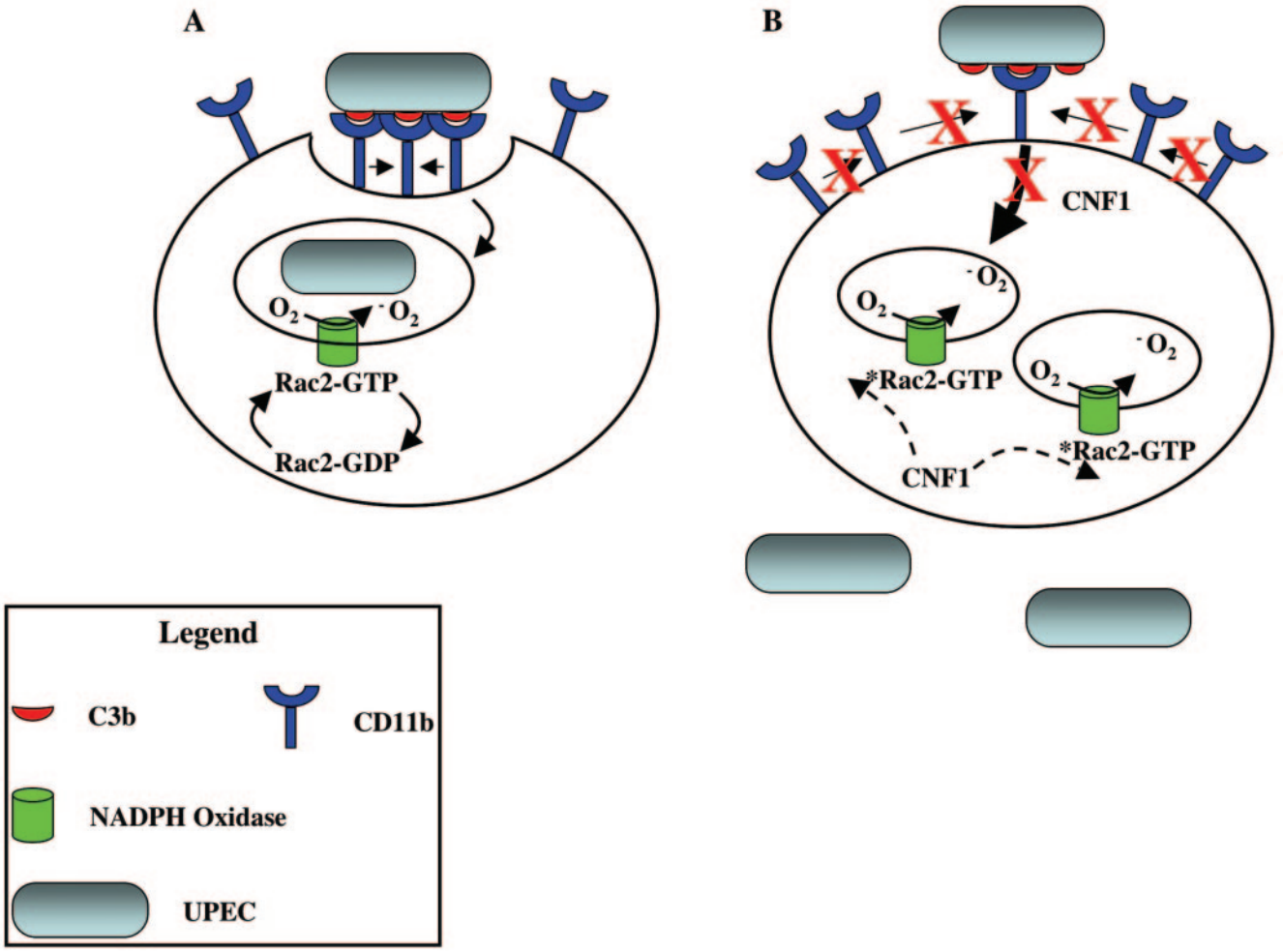

FIG. 5. Proposed model for CNF1 modulation of PMN function. (A) PMN interaction with CNF1-negative UPEC results in membrane remodeling and clustering of CD11b followed by phagocytosis of opsonized UPEC. After the PMN phagocytose the bacteria, the NADPH oxidase complex generates reactive oxygen species that inactivates the internalized UPEC strain. (B) CNF1-expressing UPEC escape the antimicrobial properties of PMNs by impairing membrane remodeling and clustering of CD11b, events that prevent the phagocytosis of opsonized UPEC. Simultaneously, CNF1 enhances the intracellular generation of reactive oxygen species independently of phagocytosis by increasing the amount of Rac2-GTP. Dashed arrows indicate the hypothesized deamidation and constitutive activation of Rac2.

receptors were not in the correct conformation to interact with serum-opsonized UPEC it is unlikely that we could have observed either greater numbers of associated UPEC compared to the isogenic mutant at any time point or an increase in the number of associated UPEC throughout the experiment.

The apparent inhibition of further phagocytosis by PMNs associated with CNF1-positive strains was not a consequence of insufficiently opsonized bacteria because the similarly treated *cnf1* mutant bacteria continued to associate with PMNs and were phagocytosed to a greater extent throughout the experiment. We believe a more reasonable explanation for the apparent inhibition of further phagocytosis by PMNs of CNF1-positive UPEC is that the concentration of CNF1 increased in our experimental system over time as the population of UPEC expanded. Thus, we speculate that the PMNs were continuously exposed to CNF1, which, in turn, led to decreased phagocytosis of the toxin-expressing organisms.

That CNF1-expressing UPEC exert an antiphagocytic effect on mouse PMNs is consistent with the conclusion of Hofman et al. (15). These researchers used flow cytometric analysis to examine phagocytic uptake of a nonpathogenic, GFP-expressing strain of *E. coli* by human PMNs intoxicated 18 to 24 h prior to bacterial exposure with CNF1. Hofman and colleagues showed that purified CNF1 inhibits phagocytosis by such CNF1-treated PMNs. Our results on the impact of CNF1 on phagocytosis of PMNs are in keeping with these data and extend the findings to show that the antiphagocytic effect of CNF1 can occur coincident with exposure to CNF1-expressing UPEC.

The greater net growth of the serum-opsonized, CNF1-positive wild-type strain and complemented clone compared to serum-opsonized *cnf1* mutant bacteria when coincubated with PMNs was negated when serum was heat inactivated or when cytochalasin D was present. The obliteration of this differential replication effect indicates that heat-labile factors and phagocytosis are required for the control of both CNF1-positive and CNF1-negative UPEC. Heat-labile factors such as complement can opsonize bacteria that are then recognized by com-

plement receptors such as complement receptor 3 on the surface of PMNs. The recognition of opsonized bacteria by and clustering of CR3 then results in the phagocytosis of complement-opsonized bacteria.

Consistent with the requirement for CR3 clustering beneath opsonized bacteria, we observed by confocal microscopy that CR3 did not aggregate beneath bacteria when PMNs were exposed to CNF1-expressing UPEC. However, clustering of CR3 did occur in PMNs coincubated with CP9*cnf1*. In contrast to our results, Hofman demonstrated that CNF1 intoxication of human PMNs resulted in many punctate patches of CR3 (15). The reason our results and those of Hofman and colleagues are at variance may reflect our different experimental strategies. We used a UPEC-PMN infection model and examined early time points, while Hofman and coworkers intoxicated the PMNs with CNF1 and then assessed CD11b clustering at later time points. In addition, the PMNs used in our experiments were likely at a different state of activation when exposed to UPEC then the human PMNs purified by Hofman and colleagues from venous blood. Other aspects of our results were similar to those of Hofman and coworkers; for example, we also did not detect any difference in the amount of CR3 exposed on the surface of the PMN.

Precisely how CNF1 affects the distribution of CR3 is not clear, but it is known that the Rho GTPases that are targets of CNF1 can influence the avidity maturation of integrins (33), possibly by controlling the polymerization state of actin (19). Indeed, Kucik and colleagues (19) showed that increased lateral mobility of the β_2 integrin LFA-1 could be explained by the release of LFA-1 from its cytoskeletal constraints by depolymerization of actin with cytochalasin D. The release of LFA-1 was accompanied by a 10-fold increase in lateral mobility and increased adhesion to ICAM-1.

We also demonstrated that CNF1-expressing UPEC developed a more robust luminol dependent chemiluminescent signal compared to the CNF1-negative strain, a finding that indicates that the intracellular generation of reactive oxygen species was increased compared to the isogenic mutant. The finding that intracellular reactive oxygen species generation was increased in spite of a decrease in phagocytic capacity is at first counterintuitive. However, we believe that both the increase in intracellular reactive oxygen species and diminished phagocytic capacity are the result of CNF1 activity on Rho family members in PMNs. Our detection of increased Rac2-GTP in PMNs exposed to CNF1-expressing UPEC provides an explanation for the observed reactive oxygen species increase in our model.

The NADPH oxidase complex was the first characterized Rho GTPase-regulated system (4). That Rac2 can regulate the NADPH oxidase complex required for generation of reactive oxygen species was demonstrated in a cell-free system with Rac2 purified from human PMNs (18). Additional support for the role of Rac2 in the oxidase was provided by animal and human studies (1, 14, 20, 24). Thus, our results are consistent with the recognized role of Rac2 in NADPH oxidase assembly and reactive oxygen species generation and support and extend the findings of Hofman et al., who showed that purified CNF1 enhances the production of reactive oxygen species in PMNs (15). In our experimental system, the observed increase in intracellular reactive oxygen species generation can be viewed as a consequence of toxin activity that led to increased levels of Rac2-GTP rather than from increased PMN phagocytic capacity.

In spite of the large increase in intracellular reactive oxygen species in PMNs exposed to CNF1-producing UPEC, no increased release of reactive oxygen species into the extracellular environment was detected. The finding that extracellular levels of reactive oxygen species were similar for PMNs exposed to CNF1-positive and CNF1-negative UPEC was surprising and suggests that intoxicated PMNs are unable to deliver the intracellular reactive oxygen species to the extracellular environment. The accumulation of extracellular reactive oxygen species has been hypothesized to aid in the inactivation of bacteria that are poorly phagocytosed by PMNs (25). Therefore, by blocking this aspect of phagocyte physiology, CNF1-expressing UPEC may avoid oxidative killing by PMNs.

Our findings of increased Rac2-GTP are consistent with the result of Pop et al. who demonstrated that CNF1 may be capable of modifying Rac2 (27). Pop et al. made the additional finding that activated Rac2 in CNF1-intoxicated cells is not degraded by the proteosome as is Rac1 (27). The degradation of modified Rac1 would limit the extent of signaling by Rac1-GTP in a cell intoxicated by CNF1. If activated Rac2 is not degraded, it could participate in prolonged signaling events such as enhanced assembly of the NADPH oxidase. Such an event could, in turn, result in the increased generation of reactive oxygen species as was observed in this study.

In aggregate, our data have led us to propose the model depicted in Fig. 5. In our model, CNF1-expressing UPEC modulate key aspects of PMN physiology, in part by altering Rho-GTPase activity, leading to enhanced replication of these bacterial strains. Specifically, CNF1-expressing UPEC decrease the extent of membrane remodeling and CD11b clustering, events that result in a decreased phagocytic capacity while simultaneously increasing the extent of Rac2-GTP in PMNs. This increase in activated Rac2 then promotes an enhanced intracellular respiratory burst.

In sum, we propose that the capacity of CNF1-expressing UPEC to reduce phagocytosis by PMNs and to limit the release of reactive oxygen species allows the bacteria to survive the acute inflammatory response and facilitates enhanced net replication of the organisms. Such an expanding bacterial population in an otherwise sterile site may allow deeper tissue penetration by these strains.

ACKNOWLEDGMENTS

This work was supported by grant AI38281 from the National Institutes of Health.

We thank Hank Lockman (Battelle Memorial Institute) for plasmid pHLK140, Brian Schaefer for his help with confocal imaging and analysis, and Karen Wolcott for her assistance with flow cytometry.

The opinions or assertions contained herein are those of the authors and are not to be construed as the views of the Department of Defense.

REFERENCES

1. **Ambruso, D. R., C. Knall, A. N. Abell, J. Panepinto, A. Kurkchubasche, G. Thurman, C. Gonzalez-Aller, A. Hiester, M. deBoer, R. J. Harbeck, R. Oyer, G. L. Johnson, and D. Roos.** 2000. Human neutrophil immunodeficiency syndrome is associated with an inhibitory Rac2 mutation. Proc. Natl. Acad. Sci. USA **97:**4654–4659.
2. **Blanco, J., M. Blanco, M. P. Alonso, J. E. Blanco, E. A. Gonzalez, and J. I. Garabal.** 1992. Characteristics of haemolytic Escherichia coli with particular reference to production of cytotoxic necrotizing factor type 1 (CNF1). Res. Microbiol. **143:**869–878.

3. **Bokoch, G. M.** 1995. Regulation of the phagocyte respiratory burst by small GTP-binding proteins. Trends Cell Biol. **5:**109–113.
4. **Bokoch, G. M., and B. A. Diebold.** 2002. Current molecular models for NADPH oxidase regulation by Rac GTPase. Blood **100:**2692–2696.
5. **Bylund, J., M. Samuelsson, L. V. Collins, and A. Karlsson.** 2003. NADPH-oxidase activation in murine neutrophils via formyl peptide receptors. Exp. Cell Res. **282:**70–77.
6. **Caprioli, A., V. Falbo, L. G. Roda, F. M. Ruggeri, and C. Zona.** 1983. Partial purification and characterization of an *Escherichia coli* toxic factor that induces morphological cell alterations. Infect. Immun. **39:**1300–1306.
7. **Caron, E., and A. Hall.** 1998. Identification of two distinct mechanisms of phagocytosis controlled by different Rho GTPases. Science **282:**1717–1721.
8. **Connell, I., W. Agace, P. Klemm, M. Schembri, S. Marild, and C. Svanborg.** 1996. Type 1 fimbrial expression enhances Escherichia coli virulence for the urinary tract. Proc. Natl. Acad. Sci. USA **93:**9827–9832.
9. **Falbo, V., M. Famiglietti, and A. Caprioli.** 1992. Gene block encoding production of cytotoxic necrotizing factor 1 and hemolysin in *Escherichia coli* isolates from extraintestinal infections. Infect. Immun. **60:**2182–2187.
10. **Foxman, B.** 2002. Epidemiology of urinary tract infections: incidence, morbidity, and economic costs. Am. J. Med. **113**(Suppl. 1A)**:**5S–13S.
11. **Foxman, B., L. Zhang, K. Palin, P. Tallman, and C. F. Marrs.** 1995. Bacterial virulence characteristics of Escherichia coli isolates from first-time urinary tract infection. J. Infect. Dis. **171:**1514–1521.
12. **Gardiner, E. M., K. N. Pestonjamasp, B. P. Bohl, C. Chamberlain, K. M. Hahn, and G. M. Bokoch.** 2002. Spatial and temporal analysis of Rac activation during live neutrophil chemotaxis. Curr. Biol. **12:**2029–2034.
13. **Goullet, P., B. Picard, M. Contrepois, J. De Rycke, and J. Barnouin.** 1994. Correlation between esterase electrophoretic polymorphism and virulence-associated traits in extra-intestinal invasive strains of Escherichia coli. Epidemiol. Infect. **112:**51–62.
14. **Gu, Y., B. Jia, F. C. Yang, M. D'Souza, C. E. Harris, C. W. Derrow, Y. Zheng, and D. A. Williams.** 2001. Biochemical and biological characterization of a human Rac2 GTPase mutant associated with phagocytic immunodeficiency. J. Biol. Chem. **276:**15929–15938.
15. **Hofman, P., G. Le Negrate, B. Mograbi, V. Hofman, P. Brest, A. Alliana-Schmid, G. Flatau, P. Boquet, and B. Rossi.** 2000. Escherichia coli cytotoxic necrotizing factor-1 (CNF-1) increases the adherence to epithelia and the oxidative burst of human polymorphonuclear leukocytes but decreases bacteria phagocytosis. J. Leukoc Biol. **68:**522–528.
16. **Kaper, J. B., J. P. Nataro, and H. L. Mobley.** 2004. Pathogenic Escherichia coli. Nat. Rev. Microbiol. **2:**123–140.
17. **Kim, C., and M. C. Dinauer.** 2001. Rac2 is an essential regulator of neutrophil nicotinamide adenine dinucleotide phosphate oxidase activation in response to specific signaling pathways. J. Immunol. **166:**1223–1232.
18. **Knaus, U. G., P. G. Heyworth, B. T. Kinsella, J. T. Curnutte, and G. M. Bokoch.** 1992. Purification and characterization of Rac 2. A cytosolic GTP-binding protein that regulates human neutrophil NADPH oxidase. J. Biol. Chem. **267:**23575–23582.
19. **Kucik, D. F., M. L. Dustin, J. M. Miller, and E. J. Brown.** 1996. Adhesion-activating phorbol ester increases the mobility of leukocyte integrin LFA-1 in cultured lymphocytes. J. Clin. Investig. **97:**2139–2144.
20. **Kurkchubasche, A. G., J. A. Panepinto, T. F. Tracy, Jr., G. W. Thurman, and D. R. Ambruso.** 2001. Clinical features of a human Rac2 mutation: a complex neutrophil dysfunction disease. J. Pediatr. **139:**141–147.
21. **Laestadius, A., A. Richter-Dahlfors, and A. Aperia.** 2002. Dual effects of Escherichia coli alpha-hemolysin on rat renal proximal tubule cells. Kidney Int. **62:**2035–2042.
22. **Lerm, M., G. Schmidt, and K. Aktories.** 2000. Bacterial protein toxins targeting rho GTPases. FEMS Microbiol. Lett. **188:**1–6.
23. **Lerm, M., J. Selzer, A. Hoffmeyer, U. R. Rapp, K. Aktories, and G. Schmidt.** 1999. Deamidation of Cdc42 and Rac by *Escherichia coli* cytotoxic necrotizing factor 1: activation of c-Jun N-terminal kinase in HeLa cells. Infect. Immun. **67:**496–503.
24. **Li, S., A. Yamauchi, C. C. Marchal, J. K. Molitoris, L. A. Quilliam, and M. C. Dinauer.** 2002. Chemoattractant-stimulated Rac activation in wild-type and Rac2-deficient murine neutrophils: preferential activation of Rac2 and Rac2 gene dosage effect on neutrophil functions. J. Immunol. **169:**5043–5051.
25. **Lock, R., C. Dahlgren, M. Linden, O. Stendahl, A. Svensbergh, and L. Ohman.** 1990. Neutrophil killing of two type 1 fimbria-bearing *Escherichia coli* strains: dependence on respiratory burst activation. Infect. Immun. **58:**37–42.
26. **Mills, M., K. C. Meysick, and A. D. O'Brien.** 2000. Cytotoxic necrotizing factor type 1 of uropathogenic *Escherichia coli* kills cultured human uroepithelial 5637 cells by an apoptotic mechanism. Infect. Immun. **68:**5869–5880.
27. **Pop, M., K. Aktories, and G. Schmidt.** 2004. Isotype-specific degradation of Rac activated by the cytotoxic necrotizing factor 1. J. Biol. Chem. **279:**35840–35848.
28. **Rest, R. F., and D. P. Speert.** 1994. Measurement of nonopsonic phagocytic killing by human and mouse phagocytes. Methods Enzymol. **236:**91–108.
29. **Rippere-Lampe, K. E., M. Lang, H. Ceri, M. Olson, H. A. Lockman, and A. D. O'Brien.** 2001. Cytotoxic necrotizing factor type 1-positive *Escherichia coli* causes increased inflammation and tissue damage to the prostate in a rat prostatitis model. Infect. Immun. **69:**6515–6519.
30. **Rippere-Lampe, K. E., A. D. O'Brien, R. Conran, and H. A. Lockman.** 2001. Mutation of the gene encoding cytotoxic necrotizing factor type 1 (cnf(1)) attenuates the virulence of uropathogenic *Escherichia coli*. Infect. Immun. **69:**3954–3964.
31. **Russo, T. A., and J. R. Johnson.** 2003. Medical and economic impact of extraintestinal infections due to Escherichia coli: focus on an increasingly important endemic problem. Microbes Infect. **5:**449–456.
32. **Schmidt, G., P. Sehr, M. Wilm, J. Selzer, M. Mann, and K. Aktories.** 1997. Gln 63 of Rho is deamidated by Escherichia coli cytotoxic necrotizing factor-1. Nature **387:**725–729.
33. **Schwartz, M. A., and S. J. Shattil.** 2000. Signaling networks linking integrins and rho family GTPases. Trends Biochem. Sci. **25:**388–391.
34. **Underhill, D. M., and A. Ozinsky.** 2002. Phagocytosis of microbes: complexity in action. Annu. Rev. Immunol. **20:**825–852.
35. **Witko-Sarsat, V., P. Rieu, B. Descamps-Latscha, P. Lesavre, and L. Halbwachs-Mecarelli.** 2000. Neutrophils: molecules, functions and pathophysiological aspects. Lab. Investig. **80:**617–653.
36. **Yamamoto, S., T. Tsukamoto, A. Terai, H. Kurazono, Y. Takeda, and O. Yoshida.** 1995. Distribution of virulence factors in Escherichia coli isolated from urine of cystitis patients. Microbiol. Immunol. **39:**401–404.

Editor: J. T. Barbieri